Grain-Boundary Structure and Precipitation in Sensitized Austenitic Stainless Steel

Hiroyuki Kokawa, Masayuki Shimada, and Yutaka S. Sato

Grain-boundary carbide precipitation and intergranular corrosion in sensitized austenite stainless steel were examined by transmission electron microscopy to clarify the effect of grain-boundary structure on precipitation and corrosion. The propensity to intergranular precipitation depends strongly on the grain-boundary structure. Carbide precipitates tend to be detected at grain boundaries with higher Σ values or larger deviation angles ($\Delta\theta$) from low-Σ coincidence site lattice misorientations. The more ordered boundary requires a longer time for intergranular carbide precipitation and corrosion than less ordered or random boundaries.

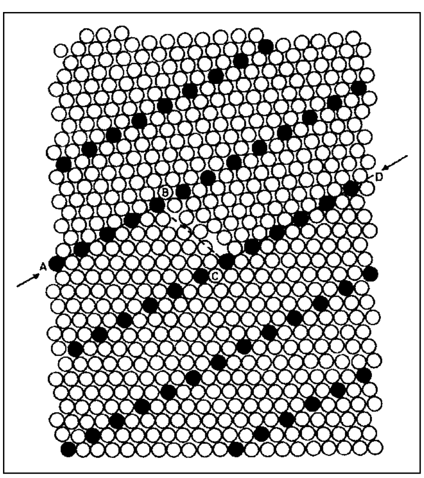

Figure 1. A two-dimensional atomic configuration at a $\Sigma 11$ CSL grain boundary with 50.5°/[110].[8]

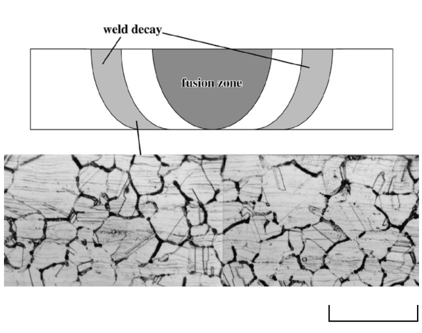

Figure 2. A mixed structure of sensitized and unsensitized boundaries in the weld decay region of a weld-heat-affected zone of austenitic stainless steel.

INTRODUCTION

One of the major reasons for intergranular corrosion in austenitic stainless steel is chromium depletion due to chromium-carbide precipitation at grain boundaries. Several techniques have been suggested to avoid intergranular corrosion, such as reducing the carbon content in the material and adding titanium, niobium, or zirconium for stabilization. Recent grain-boundary structure studies have shown that grain-boundary phenomena (such as grain-boundary diffusion,[1] precipitation,[2,3] and corrosion[4,5]) strongly depend on the grain-boundary crystallographic nature and atomic structure.[6]

Friedel[7] first showed that for certain misorientations about rotational axes there exist superlattices on which a fraction ($1/\Sigma$) of the lattice points in the two crystal lattices lie. This is referred to as a coincidence site lattice (CSL) and is independent of the interfacial plane.[6] The highest possible degree of coincidence in the cubic system, apart from a perfect crystal, is for a simple twin for which $\Sigma = 3$.[6] Figure 1 shows a CSL with $\Sigma = 11$ by a rotation of 50.5° about [110] in a body-centered cubic bicrystal as a more general example,[8] where coincident sites are indicated by solid circles. CSL boundaries should show good atomic fit.[8,9] The best fit and, hence, lowest energy occurs when the interface follows a plane containing a high density of coincidence sites, so that the boundary plane will be stepped to follow a path to maximize the proportion of good matching.[6,8] A CSL with low Σ leads to ordered boundaries at which the atomic configuration is regular and ordered.

Time-temperature-transformation and time-temperature-precipitation curves reported for austenitic stainless steels indicated that twin boundaries are not susceptible to carbide precipitation and corrosion because atomic structure is highly regular and coherent as compared to other high-angle grain boundaries.[10,11] Trillo and Murr[12,13]

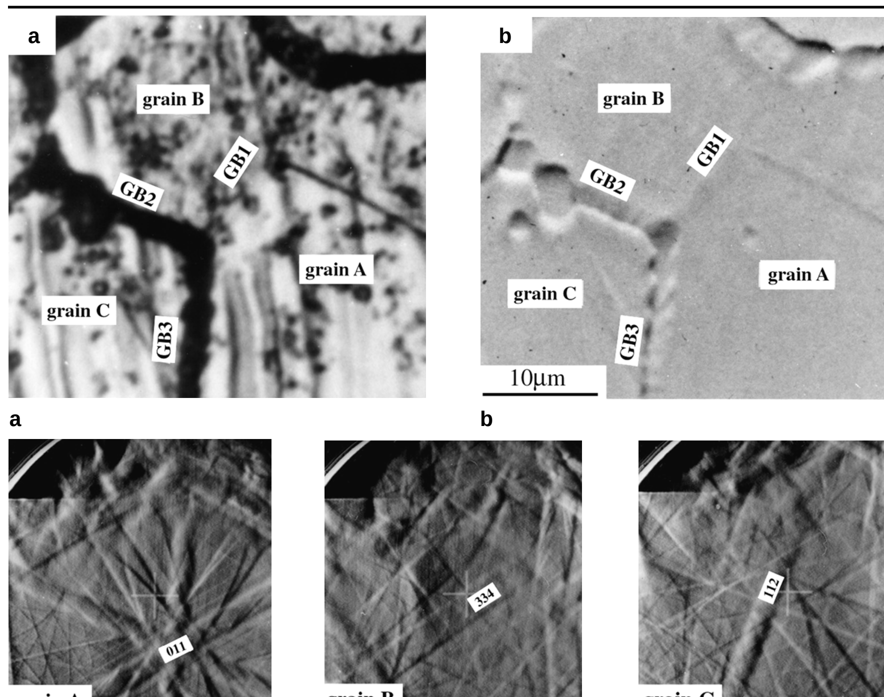

Figure 3. (a) Optical and (b) SEM micrographs of grain boundaries in the weld-decay region of 304 steel after 10% oxalic acid etching, and ECPs obtained from (c) grain A, (d) grain B, and (e) grain C.

have shown remarkable resistance of the coherent twin boundary to carbide precipitation because of extreme low boundary energy. After brief exposure to a sensitizing temperature, such as in welding, an austenitic stainless steel has a mixed structure of sensitized and unsensitized boundaries (Figure 2).[14] This suggests that each grain boundary has its own sensitivity, depending on the grain-boundary nature and structure (atomic regularity at the boundary), and short-time sensitization, such as weld decay,[15] can be inhibited by controlling grain-boundary nature and structure in the material. The purpose of this study is to make clear the relationship between grain-boundary sensitization and structure in an austenitic stainless steel according to the CSL theory[6] and to suggest that suitable grain-boundary design and control,[16–19] such as as by a proprietary thermomechanical process,[20] can prevent weld decay in stainless steels.

GRAIN-BOUNDARY SENSITIZATION AND CHARACTERIZATION

A type 304 austenitic stainless steel with the chemical composition (in wt.%) Fe-18.28Cr-8.48Ni-0.60Si-1.00Mn-0.055C-0.029P-0.005S was heat-treated at temperatures of 800–1,300 K for 10–$10^{4.5}$ s. The specimens were examined by ten percent oxalic acid-etch and Strauss tests, and by scanning and transmission electron miscroscopy (SEM

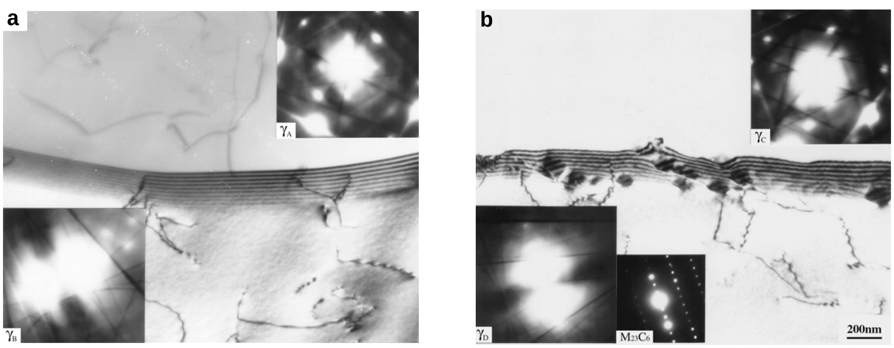

a b

Figure 4. Grain-boundary TEM structures of (a) Σ9 and (b) random boundaries in the weld-decay region of 304 steel.

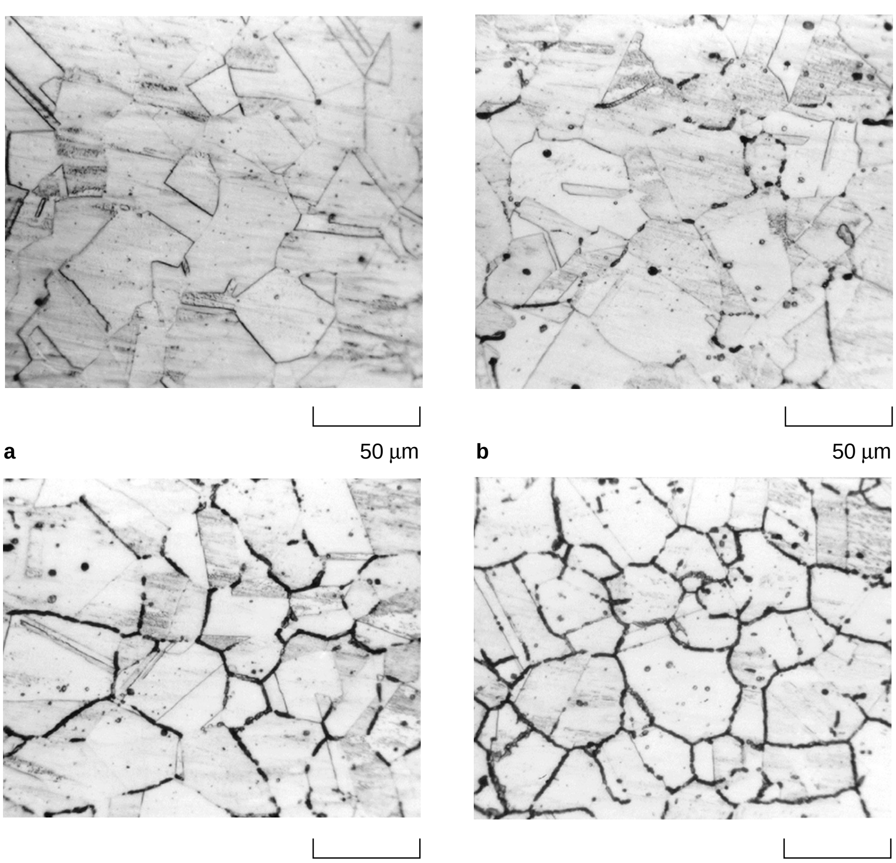

Figure 5. Optical microstructures of 304 steel that were heat-treated at 1,000 K for (a) 0 s, (b) 100 s, (c) 1,000 s, and (d) 10,000 s.

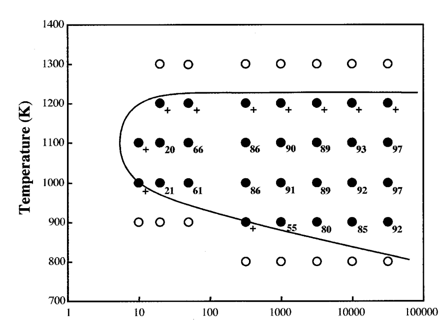

Figure 6. The time-temperature-precipitation diagram for intergranular carbide in 304 steel after an oxalic acid-etch test.

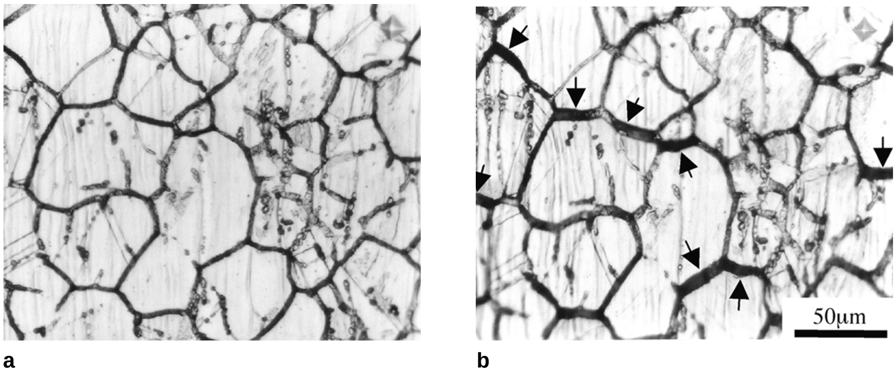

Figure 7. Oxalic acid-etched and Strauss-tested specimens heat-treated at 1,000 K for 1,000 s (a) before and (b) after a bend test.

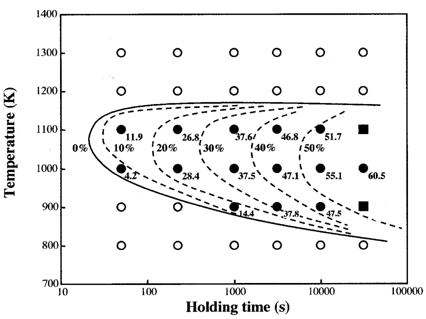

Figure 8. The time-temperature-intergranular corrosion diagram for 304 steel after a Strauss test.

and TEM). The crystallographic orientation in each grain was determined by electron diffraction channeling (ECP) and Kikuchi patterns.

The grain boundaries were characterized on the basis of CSL theory[21] using misorientation matrices;[22–27] the deviation angle $\Delta\theta$ from the nearest-Σ CSL orientation relationship was given as the rotation angle of deviation matrix, Md, from the misorientation matrix at a grain boundary.[28] The maximum deviation angle, $\Delta\theta c$, which can be accommodated in a Σ boundary by introducing grain-boundary structural dislocations, is given by Brandon's criterion, $\Delta\theta c = 15\,\Sigma^{-1/2}$ in degrees.[29] A parameter $\Delta\theta/\Delta\theta c$ was used to evaluate grain-boundary regularity.[30–32] The regularity of grain-boundary structure is considered to decrease with an increase in Σ value, because the density of CSL points in the two crystal lattices decreases.[6] CSL boundaries with $\Sigma \leq 29$ were regarded as ordered boundaries.

GRAIN-BOUNDARY STRUCTURE DEPENDENCE ON PRECIPITATION

Figure 3 shows grain boundaries in the weld-decay region of 304 steel after 10% oxalic acid etching. The grain boundary GB1 with no groove is characterized as a $\Sigma5$ CSL boundary ($\Delta\theta/\Delta\theta c$ = 0.38), while deeply grooved GB2 and GB3 are random boundaries ($\Delta\theta/\Delta\theta c$ = 1.76 and 2.27). TEM observations in the weld-decay region have revealed that some grain boundaries accept precipitation, but others do not. For example, no precipitation is seen at the grain boundary in Figure 4a, while $M_{23}C_6$ precipitates are observed at the grain boundary in Figure 4b. Their misorientations indicate that they are a $\Sigma9$ boundary in Figure 4a and a random boundary in Figure 4b.

Figure 5 shows optical microstructures of heat-treated specimens at 1,000 K after 10% oxalic acid etching. The frequency of grooved boundaries increases with the holding time at 1,000 K. The time-temperature-intergranular carbide precipitation diagram given by 10% oxalic acid etching is shown in Figure 6. Solid circles indicate that grooved boundaries were observed in the specimen. The numbers beside the solid circles correspond to the number ratio (in percentage) of grooved boundaries to all boundaries in the specimen excluding twin boundaries, and a + sign means discontinuous grooves at boundaries, as seen in Figure 5b. The frequency of intergranular carbide precipitation increases with the holding time at every temperature.

Figure 7 shows optical microstructures of a Strauss-tested specimen heat-treated at 1,000 K for 1,000 s. The specimen was oxalic-acid etched prior to testing. The microstructures were obtained from the same area before and after a bend test, respectively. Some of the grain boundaries were cracked by testing, as shown by arrows in Figure 7b.

Figure 8 is the time-temperature-corrosion diagram given by the Strauss test of the heat-treated specimens. Solid symbols indicate that cracked boundaries were detected after the bend test. The frequency of cracked boundaries is shown (in percentage) beside the solid circles (excluding twin boundaries). Solid squares mean that the specimen was fractured during the bend test. The frequency of cracked boundaries also increases with the holding time at every temperature. These diagrams suggest that the time required for carbide precipitation and corrosion depends on the grain-boundary character at sensitizing temperatures. Stickler et al.[9] and Cíhal et al.[10] reported that general high-angle (random) grain boundaries need shorter time for

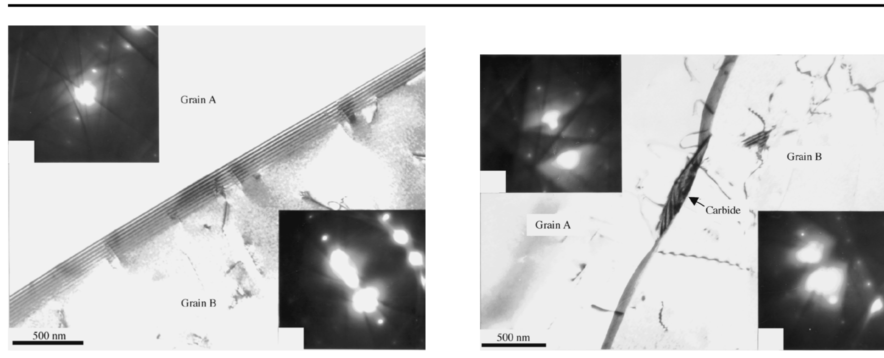

Figure 9. TEM micrographs of grain boundary structures deviated (a) 7.25 degrees and (b) 12.72 degrees from the $\Sigma9$ CSL orientation relationship in 304 steel heat-treated for 100 s at 1,000 K.

carbide precipitation and corrosion than twin boundaries. However, Figures 5 and 7 indicate that the time is different even among general high-angle boundaries, suggesting that the time may depend on the grain-boundary structure.

Figures 9 shows grain-boundary structures as revealed by TEM in a specimen heat-treated at 1,000 K for 100 s. Intergranular carbide precipitation is detected at the grain boundary in Figure 9b, but not at the grain boundary in Figure 9a. Grain-boundary characterization with Kikuchi patterns revealed that the nearest CSL relationship is $\Sigma 9$ for both grain boundaries, but the values of $\Delta\theta/\Delta\theta c$ are 1.45 and 2.54 for the grain boundaries in Figure 9a and 9b, respectively. The grain boundary with the smaller $\Delta\theta/\Delta\theta c$ has no carbide.

Figure 10 shows the borderlines[33] between grain-boundary precipitation and no precipitation during sensitization at 1,000 K for 10^2–$10^{4.5}$. In the figure, the Σ value of the nearest CSL is taken as abscissa, and the deviation angle $\Delta\theta$ from the CSL is the vertical axis. Increases in $\Delta\theta$ and Σ value mean decreases in the regularity of grain-boundary structure.[6] The grain boundaries with lower regularities in the region above the borderline accept intergranular precipitation at the holding time. The borderlines can be described by $\Delta\theta/\Delta\theta c$ (i.e., $\Delta\theta/\Delta\theta c$ = 2.4, 2.0, 1.4, and 0.3 for 100 s, 320 s, 1,000 s, and 32,000 s, respectively). The figure reveals that a more ordered boundary needs longer time for carbide precipitation and corrosion than a less ordered boundary. This tendency may result from more difficult nucleation and a lower growth rate of carbide at a more ordered boundary because of lower grain-boundary energy.

At 1,000 K, the $\Delta\theta/\Delta\theta c$ decreases with an increase in holding time. If the grain-boundary structure could be kept smaller than the $\Delta\theta/\Delta\theta c$ by grain-boundary engineering,[19,20] intergranular precipitation and corrosion would not occur. The $\Delta\theta/\Delta\theta c$ is much larger than one at a short holding time (about 2.5 at 100 s and 2 for 500 s); the character as a Σ boundary may be valid with somewhat larger deviations than Brandon's criterion for a shorter time sensitization. This suggests that the conditions to prevent intergranular carbide precipitation by controlling grain-boundary character are not very severe for a short-time exposure to a sensitizing temperature, such as in welding thermal cycles. Grain-boundary engineering[19] could inhibit the weld decay of austenitic materials.

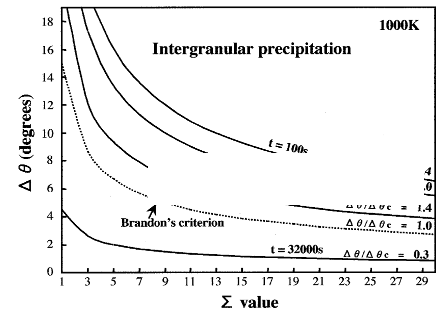

Figure 10. Intergranular carbide precipitation and the deviation angle from the CSL relationship in 304 steel during sensitization at 1,000 K.

ACKNOWLEDGEMENTS

This work was supported by the Grant-in-Aid for COE Research (No. 11CE2003); the Ministry of Education, Science, Sports and Culture; and the Japan Atomic Energy Research Institute Nuclear Research Promotion Program. The authors thank T. Wata-nabe for his useful advice, and A. Honda for his technical assistance. Financial support from Kawasaki Steel 21st Century Foundation is gratefully acknowledged.

References

1. I. Kaur and W. Gust, *Fundamentals of Grain and Interphase Boundary Diffusion* (Stuttgart, Germany: Ziegler Press, 1988), p. 275.
2. J. Le Coze et al., *Memoires Scientifiques Review de Metallurgie*, 70 (1973), p. 397.
3. J. Le Coze and M. Biscondi, *Canadian Metallurgical Quarterly*, 13 (1974), p. 59.
4. M. Froment, *J. Physique*, 36 (1975), p. c4-371.
5. X.R. Qian and Y.T. Chou, *Philosophical Magazine A*, 45 (1982), p. 1075.
6. P.H. Pumphrey, *Grain Boundary Structure and Properties*, ed. G.A. Chadwick and D.A. Smith (London: Academic Press, 1976), p. 139.
7. G. Friedel, *Leçons de Crystallographie* (Paris: Berger-Levrault Publishers, 1926).
8. D.G. Brandon et al., *Acta Metallurgica*, 12 (1964), p. 813.
9. M.L. Kronberg and F.H. Wilson, *Trans. AIME*, 185 (1949), p. 501.
10. R. Stickler and A. Vinckier, *Memoires Scientifiques Review de Metallurgie*, 60 (1963), p. 489.
11. V. Cíhal and I. Kašová, *Corr. Sci.*, 10 (1970), p. 875.
12. E.A. Trillo and L.E. Murr, *J. Mater. Sci.*, 33 (1998), p. 1263.
13. E.A. Trillo and L.E. Murr, *Acta Materialia*, 47 (1999), p. 235.
14. T. Kuwana and H. Kokawa, *Trans. Japan Welding Soc.*, 16 (1985), p. 99.
15. H. Kokawa and T. Kuwana, *Trans. Japan Welding Soc.*, 23 (1992), p. 73.
16. T. Watanabe, *Res Mechanica*, 11 (1984), p. 47.
17. T. Watanabe, *Materials Forum*, 11 (1988), p. 284.
18. T. Watanabe, *Scripta Metallurgica et Materialia*, 27 (1992), p. 1497.
19. G. Palumbo, E.M. Lehockey, and P. Lin, *JOM*, 50 (2) (1998), p. 40.
20. P. Lin et al., *Scripta Metallurgica et Materialia*, 33 (1995), p. 1387.
21. W. Bollmann, *Crystal Defects and Crystalline Interfaces* (Berlin: Springer-Verlag, 1970).
22. D.H. Warrington and P. Bufalini, *Scripta Metallurgica*, 5 (1971), p. 771.
23. W. Bollmann, B. Michaut, and G. Sainfort, *physica status solidi (a)*, 13 (1972), p. 637.
24. H. Grimmer, W. Bollmann, and D.H. Warrington, *Acta Crystallography A*, 30 (1974), p. 197.
25. P.H. Pumphrey, *physica status solidi (a)*, 28 (1975), p. 545.
26. W.A. Clark and D.A. Smith, *Philosophical Magazine A*, 38 (1978), p. 367.
27. H. Kokawa, T. Watanabe, and S. Karashima, *Scripta Metallurgica*, 21 (1987), p. 839.
28. V. Randle and B. Ralph, *Journal of Materials Science*, 21 (1986), p. 3823.
29. D.G. Brandon, *Acta Metallurgica*, 14 (1966), p. 1479.
30. H. Kokawa, T. Watanabe, and S. Karashima, *Philosophical Magazine A*, 44 (1981), p. 1239.
31. H. Kokawa, T. Watanabe, and S. Karashima, *Journal of Materials Science*, 18 (1983), p. 1183.
32. H. Kokawa, T. Watanabe, and S. Karashima, *Scripta Metallurgica*, 17 (1983), p. 1155.
33. H. Kokawa et al., *Properties of Complex Inorganic Solids*, vol. II, ed. A. Meike et al. (Dordrecht, Netherlands: Kluwer Academic/Plenum Publishers, in press).

Hiroyuki Kokawa is a professor, Masayuki Shimada is a Ph.D. student, and Yutaka S. Sato is a research associate in the Department of Materials Processing at the Graduate School of Tohoku University.

For more information, contact Hiroyuki Kokawa, Aoba-yama 02, Sendai 980-8579, Japan; telephone 81-(22)-217-7351; fax 81-(22)-217-7351; e-mail kokawa@material.tohoku.ac.jp.